Evaluation of Autophagy Process in Differentiation of Human Induced Pluripotent Stem Cells toward Insulin Producing Cells

A. Sabet[1,2], N. Azarpira[3]*, L. Kohan[4], S. Ghavami[5]

[1]Department of Genetics, Fars Science and Research Branch, Islamic Azad University, Marvdasht, Iran
[2]Department of Genetics, Marvdasht Branch, Islamic Azad University, Marvdasht, Iran
[3]Transplant Research Center, Shiraz University of Medical Sciences, Shiraz, Iran
[4]Department of Biology, Arsanjan Branch, Islamic Azad University, Arsanjan, Iran
5Department of Human Anatomy and Cell Science, Rady Faculty of Health Sciences, Max Rady College of Medicine, University of Manitoba, Winnipeg, MB, Canada

ABSTRACT

Background: Autophagy is an intracellular self-degradative homeostasis process which eliminates undesirable and harmful macromolecules and organelles. Autophagy is also involved in self-renewal and differentiation of induced pluripotent stem cell (iPSCs).

Objective: In this study, we investigated the expression profile of autophagy marker genes in human iPSCs during their differentiation induction toward insulin producing β-like cells.

Methods: Human iPSC line, R1-hiPSC1, was used for differentiation induction toward β-like cells. The mRNA expression of *Nanog*, *OCT4* (pluripotency markers), *SOX17*, *FOXA2* (endodermic markers), *PTF1A*, *NKX6.1* (exocrine/endocrine determinants), and *PDX1* were measured during differentiation stages. Autophagy was monitored by genes expression study of four autophagy markers, *MAP1LC3B*, *BECN1*, *SQSTM1/P62* and *ATG5*, along with protein expression profile of LC3b-II during differentiation stages.

Results: The mRNA expression measurement of pluripotency, endoderm and exocrine/endocrine marker genes confirmed that hiPSCs skipped pluripotency, differentiated into endoderm, passed through the pancreatic lineage commitment stage and successfully generated insulin producing β-like cells. Expression profile of autophagy genes during differentiation stages indicated the decreased expression levels at the early stages (EB and MEI) and then increased at the definitive endoderm stages (DEI 1, DEI 2 and DE) followed by a subtractive pattern toward the end of differentiation. The results of protein expression of LC3b-II were consistent with gene expression data.

Conclusion: This study demonstrated the high contribution of key autophagy genes/proteins during the differentiation of hiPSC toward β-like cells. The enhanced autophagy levels were a prominent feature of early stages of differentiation and DE rather than the later stages.

KEYWORDS: Induced pluripotent cell; β-like cell; Autophagy; Differentiation

INTRODUCTION

The cell is pivotally dependent on a self-degradative catabolic process, autophagy, in order to regulate the sources of energy under critical conditions such as development and nutrient stress. Autophagy can preserve the cells from undesirable aggregated proteins and impaired organelles, and it plays a crucial role in the recycling of cytoplasmic components during tissue homeostasis [1-3]. Starvation or other quality control mechanisms can lead to the induction of autophagy regulation in multiple fundamental cellular processes including self-renewal, apoptosis, and differentiation [4-6].

*Correspondence: Negar Azarpira, MD
Transplant Research Center, Shiraz University of Medical Sciences, Shiraz, Iran
ORCID: 0000-0002-5549-0057
Tel: +98-917-3176294
E-mail: negarazarpira@yahoo.com

Table 1: Primer sequences.

Gene	Primer sequence (5'→3')	Tm (°C)	Product (BP)
BECN1	F: ATCTGGCACAGTGGACAGTTTG R: CGTAAGGAACAAGTCGGTATCTCTG	61	175
SQSTM1/P62	F: CCCCACGGCAGAATCAGCT R: CTCTGTGCTGGAACTCTCTGGAG	62.5	181
MAP1LC3B	F: ACGGGCTGTGTGAGAAAACG R: GTGAGGACTTTGGGTGTGGTT	61	82
ATG5	F: GGCCATCAATCGGAAACTC R: AGGTCTTTCAGTCGTTGTCT	58	94
GAPDH	F: GGACTCATGACCACAGTCCA R: CCAGTAGAGGCAGGGATGAT	60	119

The autophagy processes can be studied in different phases. During the initiation phase, the key regulatory complex, mammalian target of rapamycin (mTOR) which negatively regulates autophagy, is inactivated in response to stress and other autophagy stimuli which results in activation of the ULK complex [7]. This in turn induces the recruitment and activation of VPS34 complex 1 (VPS34-I) which catalyzes the conversion of the phospholipid phosphatidylinositol to phosphatidylinositol-3 phosphate (PI3P). VPS34-I consists of the catalytic subunit VPS34, the regulatory subunit Beclin1, AMBRA1, and VPS15 [6]. The phagophore extension phase recruits two ubiquitin-like conjugation mechanisms. The first mechanism conjugates ATG12 to ATG5 which then binds ATG16L. The second mechanism is the generation of LC3-II through conjugation of LC3-I to phosphatidylethanolamine (PE). LC3-II, in turn, mediates binding of autophagosomes complex to autophagic substrates. The fusion of autophagosomes with lysosomes produces autolysosomes, followed by luminal acidification and activation of lysosomal hydrolases which culminate in substrate degradation. Consequently, the degraded autolysosome contents are recycled back into the cytosol [8-10].

Type 1 diabetic patients have roughly been managed by replacement of β cells and currently, this strategy is executed by transplantation of pancreas or islet compartment of the pancreas all over the world. This approach has some limitations, including scarcity of donors, cell quality of donors, the small number of islet cell which yields from cadaveric patients, and life-long requirement of immunosuppression drugs [11, 12]. Therefore, an alternative cell source is needed for the unlimited production of pancreatic β cell.

Using hiPSC technology, researchers have been able to generate many cell types from different cell lineages [13] such as pancreatic islet cells. Differentiation of hiPSC into islet cells encompasses six stages including embryoid body (EB), definitive endoderm (DE), primitive gut (PG), posterior foregut (PF), pancreatic endoderm (PE), and insulin-producing β-like cells. The goal of this study was to monitor the autophagy levels during the differentiation induction of iPSCs toward insulin producing β-like cells.

MATERIALS AND METHODS

Cell Culture

The human iPSC line (R1-hiPSC1) was obtained from cell bank of Royan Institute (Tehran, Iran). The R1-hiPSC1 was cultured on mitomycin-C inactivated mouse embryonic fibroblasts (MEF) layer (M7949, Sigma, Germany) and supplemented with iPSC medium comprising Dulbecco's modified Eagle's medium (DMEM)/Ham's F12 (1:1; Life Technologies), 20% knockout serum replacement (KSR) (cat#10828020,Gibco), 2 mM L-glutamine (cat#G8540, Sigma-Aldrich), 0.1

Table 2: List and features of antibodies.

Antibody	Catalog Number	Company	Dilution	Blocking Buffer (Diluent)	Target size	Organism of Origin
Primary Ab						
Anti LC3b-II	L7543	Sigma	1:1000	5% w/v Skimmed milk	16–18 KDa	Rabbit
Anti-Beta-Actin	Ab8227	Abcam	1:1000	2% w/v BSA	42 KDa	Rabbit
Secondary Ab						
Anti- Rabbit IgG H&L HRP linked	Ab6721	Abcam	1:2000	2% w/v BSA		Goat

mM non-essential amino acids (cat#M7145, Sigma-Aldrich), 0.1 mM β-mercaptoethanol (cat#15433, Merck), 1X ITS (I1884 Sigma-Aldrich), 100 U/ml penicillin-100 µg/ml streptomycin (Life Technologies), and 12 ng/ml b-FGF (cat#F0291Sigma-Aldrich). Hanging drop protocol was used for EB production (as the first step of differentiation) and then subjected to differentiation as previously described by Ghorbani-Dalini et al. [14]. Gene expression and protein analysis of autophagy marker genes were performed in hiPSC and differentiated cell stages including EB, MEI, DEI 1, DEI 2, DE, PG, PF, PE and β-like cells.

Quantitative Real-time PCR

Total RNA and protein of hiPSC and differentiated cells were extracted using Allprep RNA/Protein extraction (Qiagen, USA) according to the manufacturer's instruction. The quality and concentration of RNA were evaluated by NanoDrop™ Lite Spectrophotometer (ThermoFisher Scientific, USA). In order to synthesize cDNA, Complementary DNA Synthesis Kit (Takara, Japan) was utilized according to the manufacturer's protocol and stored at -20°C. The quantitative RT-PCR (qRT-PCR) was performed using the StepOnePlus instrument (Applied Biosystem, USA). The relative mRNA expression levels were assessed by the $2^{-\Delta\Delta Ct}$ method and normalized to an internal control, where the ΔCt represents the difference between target and housekeeping (*GAPDH*) genes. The fold changes were calculated in comparison with the non-treated hiPSC line.

The amplification was carried out by a reaction mixture of 1 µl cDNA, 5 µl CYBR green master mix 2X (Takara, Japan) and 10 pM per primer (Table 1). The reaction was performed according to the following condition: initial denaturation at 95 ˚C for 30 s, followed by forty cycles at 95 ˚C for 5 s, 58-62.5 ˚C (as mentioned in Table 1) for 15 s and 72 ˚C for 20 s. The level of mRNA expression of target genes was normalized with *GAPDH* mRNA.

Western Blot Analysis

The concentration of proteins was measured by the Bradford method and Coomassie Protein Assay Kit. From each sample, 25 mg of total proteins was extracted over 12.5% sodium dodecyl sulfate-polyacrylamide gels, blocking in 2% BSA/Tris-buffered saline containing 0.1% Tween 20 (TBST buffer) overnight, and electrotransferred to PDVF membranes. The membranes were then incubated with rabbit Ab against LC3b-II (1:1000) and rabbit Ab against Beta-Actin (1:1000), at 4 °C overnight with gentle agitation (Table 2). After washing away unbound primary antibody with TBST buffer, goat-anti-rabbit IgG HRP-linked secondary antibody (1:2000) was added and the membrane incubated at 25 °C for a further 2 hrs with gentle agitation. After gently washing with TBST buffer, all immunoreactive bands were then visualized using ECL Substrate Kit. Protein band were detected by ChemiDoc XRS System (Bio-Rad) and the visible bands were then quantified using ImageJ software (NIH, Bethesda, MD).

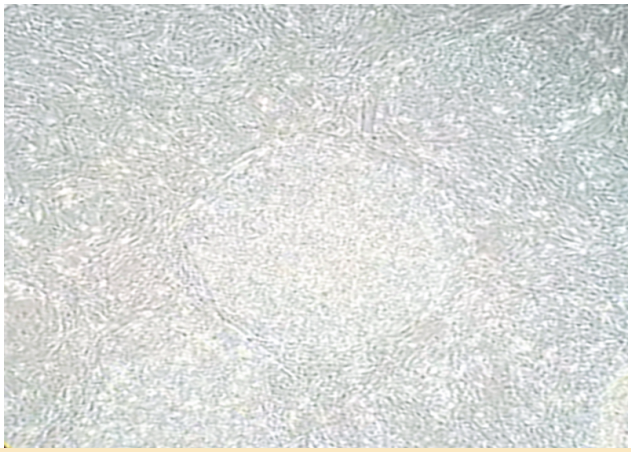

Figure 1: The R1-hiPSCs on MEF layer (using phase contrast microscopy at 10x magnifications).

Statistical Analysis

All samples were studied in triplicates. All data are presented as a mean ± SEM. One-way ANOVA was used for statistical analysis of data. Tukey-Kramer's was used as post-hoc test for comparison between each stage of differentiation. Dunnett was used as post-hoc test for statistical comparison between gene expressions of each stage with human islets. P-values less than 0.05 were considered statistically significant. The GenEX v.6.1 and GraphPad Prism v7.01 software was used for data analysis and graph plots.

RESULTS

Cell Culture

The R1-hiPSC were cultured on MEF layer and proliferated successfully. Visual observation using phase contrast microscopy at 10x magnifications confirmed typical phenotypic characteristics of undifferentiated iPSC such as compact cobblestone appearance, definite and distinct individual cell borders, as well as large nucleus with little cytoplasm (Fig 1).

mRNA Expression Pattern of Differentiated Human β-like Cells from hiPSC

Gene expression profile of β-like cells during differentiation was measured in comparison with undifferentiated hiPSC and human islet cells. Stage specific gene expression profile for *Nanog*, *OCT4*, *SOX17*, *FOXA2*, *PTF1A*, *NKX6.1*, and *PDX1* during stages of differentiation process including: iPSC, EB, DE, PG, PE and BC were expressed consistent with prior reports shown by us and others (data not shown) [14, 15].

We have previously reported [14] that analysis of *OCT4* and Nanog, as pluripotency markers, showed a stage-wise significant decrease in expression of both genes during differentiation. Moreover, analysis of *SOX17* and *FOXA2*, as endoderm markers, exhibited a steady increase in their expression. These results strongly indicated that our clusters transitioned from pluripotency stage into endoderm linage. Further investigation into expression of *PTF1A* and *NKX6.1*, as key determinants of exocrine/endocrine patterning, revealed an increase in *PTF1A* expression during early stages of differentiation. This early expression of *PTF1A* likely contributed to committing our clusters into pancreatic lineage. However, expression of *PTF1A* was suppressed at islet-like stage, while expression of *NKX6.1* increased. This provides evidence that a cross-repressive loop between *PTF1A* and *NKX6.1* directed our cluster toward endocrine cell differentiation. This reciprocal repression between *PTF1A* and *NKX6.1* genes may enable a switch in multipotent progenitors that directs progenitors to either an endocrine or acinar cell fate choice. Finally, the differentiation favoring endocrine cell commitment is confirmed by enhanced expression *PDX1* alo-

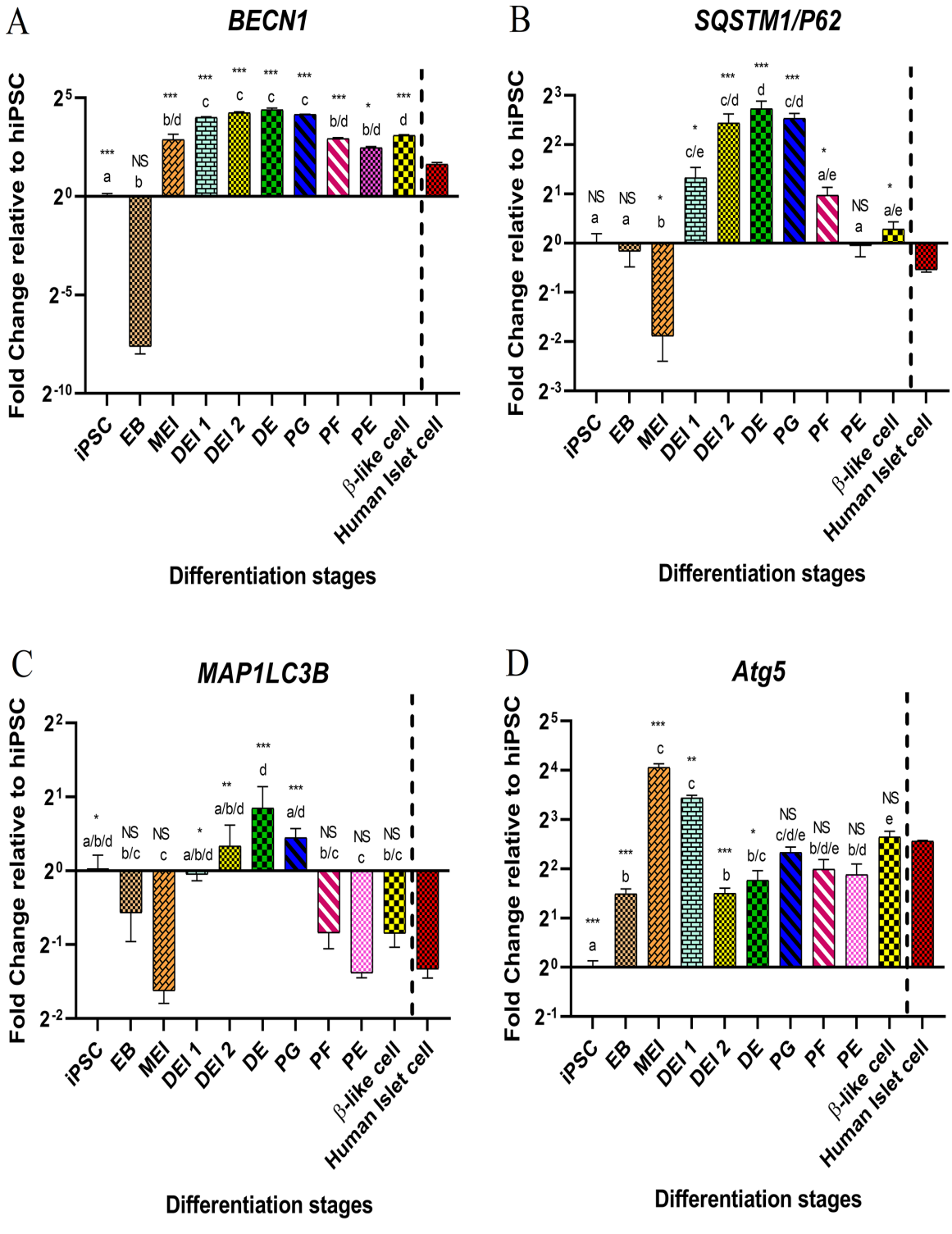

Figure 2: Dynamics of *BECN-1* (A), *SQSTM1/P62* (B), *MAP1LC3B* (C), and *ATG5* (D) mRNA expression levels during the course of differentiation. Distinct letters mean statistically significant variation between hiPSC and differentiation steps using one-way ANOVA with Tukey-Kramer's post-hoc test for multiple comparisons. Stars represent statistically significant variation for each step of differentiation versus human islet cell (*) $p<0.05$, (**) $p< 0.01$, (***) $p<0.001$. NS: Nonsignificant, EB: Embryoid body, MEI: Mesendoderm induction, DEI 1: 1th day of definitive endoderm induction, DEI 2: 2nd day of definitive endoderm induction, DE: Definitive endoderm, PG: Primitive Gut, PF: Primitive foregut, PE: Pancreatic endoderm.

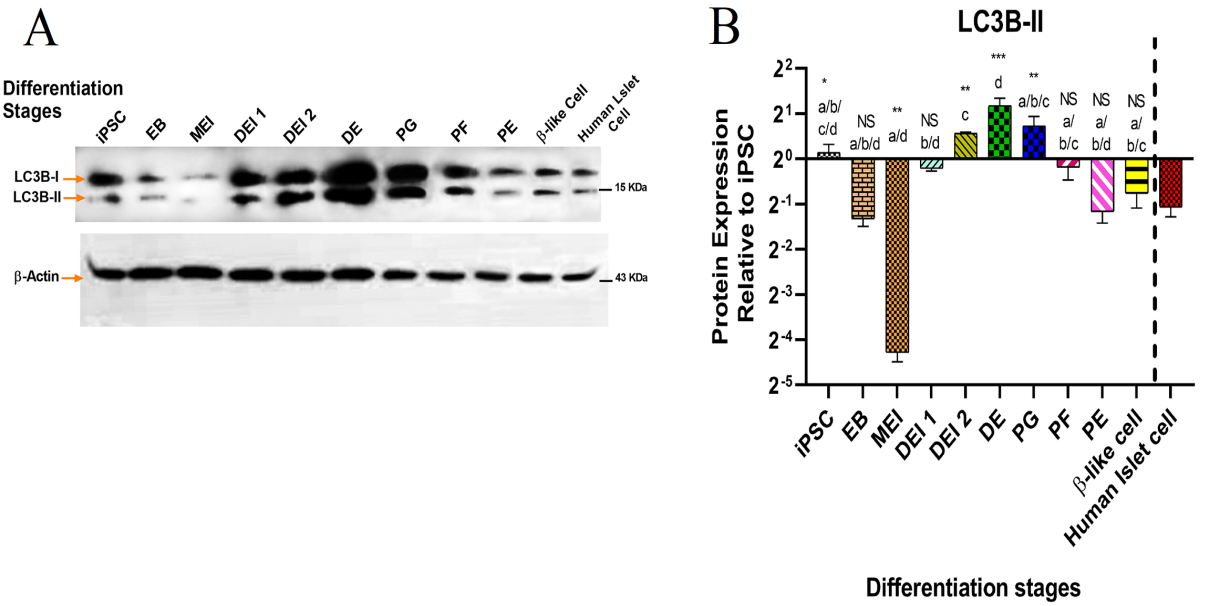

Figure 3: The western blot analysis of LC3b-II protein expression and dynamics of LC3b-II protein expression levels during different days of differentiation. EB: Embryoid body, MEI: Mesendoderm induction, DEI 1: 1th day of definitive endoderm induction, DEI 2: 2nd day of definitive endoderm induction, DE: Definitive endoderm, PG: Primitive Gut, PF: Primitive foregut, PE: Pancreatic endoderm.

ngside with *NKX6.1*, which is a key indicator of endocrine pancreas [14]. Therefore, these expression profile changes clearly indicated that hiPSCs were induced to differentiate into islet-like cells.

mRNA Expression of Autophagy Genes during Differentiation

Autophagy was monitored by investigation of mRNA expression level of *MAP1LC3B*, *BECN1*, *ATG5* and *SQSTM1/P62* during differentiation stages. The fold change ratio was quantified against iPSC. Fig 2 represent the differences in the dynamics of autophagy marker genes mRNA. We observed a considerable level of cell death and morphological changes during the early differentiation stages. Therefore, we hypothesized that maximum autophagy might occur during the definitive endoderm induction steps (DEI 1, DEI 2, and DE). Thus, six samples indicating iPSC, EB, and the early differentiation induction stages (MEI, DEI 1, DEI 2, and DE) were collected. In addition, 4 cell samples representing the rest of the differentiation process (PG, PF, PE and β-like cells) were also isolated.

The mRNA expression data indicated high baseline levels of *BECN1*, *SQSTM1/P62*, *MAP1LC3B*, and *ATG5* in iPSCs. Compared to iPSCs, *BECN1* mRNA expression down-regulated significantly in EB cells (0.005±0.001-fold $p<0.001$). During the mesendoderm induction and definitive endoderm period (MEI, DEI 1, and DEI 2) *BECN1* mRNA expression increased progressively, reaching a culmination in DE (20.96±1.29 fold; $p<0.001$) phase. However, from PG onward, *BECN1* mRNA expression was reduced (17.85±0.104; $p<0.001$) and the downward trend continued to PF (7.64±0.22; $p<0.001$) and PE (5.51±0.27; $p<0.001$) stages. This trend reversed on day 22 (β-like cells) when expression profile showed an increase in *BECN1* mRNA level (8.51±0.25; $p<0.001$) which was slightly higher relative to baseline human islet cells (3.10±0.18; $p<0.001$) (Fig 2A).

Minimal basal P62 gene expression was detected at EB and MEI cell samples (0.89±0.18; $p=0.99$, 0.27±0.08; $p<0.001$). Expression was then enhanced at MEI, DEI 1, and DEI 2, attaining a maximum level at DE (6.61±0.76; $p<0.001$). At PG stage, *P62* mRNA expres-

sion down regulated (5.79±0.40; p<0.001) which continued through PF and PE stages (1.97±0.22; p=0.24; 0.97±0.14; p=0.99). We observed a minor increase in *P62* mRNA expression by the time the cells reached β-like phase (1.21±0.13; p=0.99) (Fig 2B).

The *MAP1LC3B* mRNA expression profile followed a pattern similar to *BECN1* and *P62*. During the EB generation we observed low levels of *MAP1LC3B* mRNA expression (0.67±0.16; p=0.64), which continued with further decline until MEI (0.32±0.04; p=0.001). From DEI 1, gene expression ramped up significantly (0.97±0.05; p=1), which extended to DEI 2 and DE, when it reached its peak (1.80±0.40 fold; p=0.40). During the rest of the differentiation process, *MAP1LC3B* gene expression declined gradually until PE (PG; 1.37±0.12; p=0.94, PF; 0.56±0.08; p=0.23, PE; 0.38±0.02; p=0.009). In contrast, by β-like cell stage, samples demonstrated a feeble increase in mRNA compared to PE and human islet cells (β-like cells 0.56±0.07; p=0.25, human islet cells, 0.40±0.03; p= 0.01) (Fig 2C).

The *ATG5* mRNA expression profile showed a significant increase in EB and MEI stages (2.81±0.21; p<0.001 and 16.67±0.84; p<0.001), while in DEI stages decreased notably and reached to 3.40±0.49 (p<0.001) at DE. During the rest of differentiation stages, insignificant changes were detected. In β-like cells, a minor increase in *ATG5* mRNA expression was observed (6.27±0.50) compared to human islet cells (5.90±0.06) (Fig 2D).

Protein Expression of Autophagy Genes during Differentiation

The western blot analysis of LC3b-II conversion was consistent and correlated well with mRNA expression data (Fig 3A). The protein expression levels during the course of differentiation are presented in Fig 3B. During the EB generation, a reduction in LC3b-II protein expression was observed (0.40±0.04; p=0.297), which continued to MEI (0.05±0.007; p=0.1) stage. From DEI 1 onwards, LC3b-II protein expression increased until plateauing at DE (2.25±0.28; p=0.48). A reverse trend was noted from PG samples with a down-regulation of LC3b-II protein (1.65±0.26; p=0.88). This decline continued to PF (0.88±0.27; p=0.99) and PE (0.45±0.13; p=0.42) stages when the course changed and by β-like cell, LC3b-II protein expression was up-regulated (0.59±0.12; p=0.69) which slightly surpassed the human islet protein levels (0.48±0.65; p=0.40).

DISCUSSION

Autophagy is an evolutionarily conserved cellular degradation process that acts as an intracellular quality control mechanism through degradation of damaged or obsolete organelles and proteins. It has been proved that autophagy also plays a critical role in stem cell maintenance, cell differentiation processes, cellular reprogramming, and iPSC generation [16, 17]. Recent studies demonstrated that autophagy is responsible for the function and survival of pancreatic β cells [18]. For instance, in murine β cells, autophagy was suggested to control insulin secretion, and essential for the maintenance of homeostasis [19, 20]. However, excessive autophagy (e.g., by rapamycin treatment) has caused islet function impairment both in vitro and in vivo [21]. The essential role of autophagy during in vitro differentiation of stem cells into insulin producing cells has been reported in many studies [22-24]. In this study, we focused on establishing insulin-producing islet-like clusters from differentiated hiPSCs and evaluated the expression of autophagy marker genes during different stages of differentiation (hiPSC, EB, MEI, DEI 1, DEI 2, DE, PG, PF, PE and β-like cell). We succeeded in producing islet β-like cells from hiPSCs using our established method [14].

We evaluated the profile of differentiated hiPSCs gene expression and compared it with human islet cells. In our prior study, the pluripotency stage of cells was ascertained through expression measurement of the pluripotency markers *Nanog* and *OCT4* genes [14]. Our data concluded that our hiPSCs acquired the propensity to exit the pluripotency stage and develop into islet-like clusters. The expression of endodermic markers (*SOX17* and *FOXA2*) showed that differentiated iPSCs intersected the endoderm stage of differentiation. In addi-

tion, we observed high expression of *NKX6.1* transcription factor which plays a major role in regulation of insulin biosynthesis and secretion by β cells. A high level of *PDX1* gene expression was also observed during the differentiation of our islet-like clusters which supports our observation of the β-like cell enrichment.

To monitor the activity of autophagy process, we examined known markers including *SQSTM1/P62*, *MAP1LC3B*, *BECN1*, and *ATG5* in hiPSC-derived cells at differentiation stages [25]. Recent studies have confirmed the high levels of basal autophagy activity during iPSC derivation and maintenance[26]. Our data indicated that *MAP1LC3B* and *P62* expression decreased during EB generation. The decline in autophagy may be partly attributed to the presence of 20% FBS in the EB culture medium and an abundance of nutrients which diminishes autophagy [27]. At DEI 1, cells were subjected to 100 ng/ml Activin A and 3μM chir99021 which coincided with a decrease in autophagy levels. It has been suggested that the Wnt/β-catenin signaling pathway and autophagy are oppositely regulated [28, 29] and Chir99021 is well known Wnt signaling pathway activator [30]. Therefore it may contribute to the observed decrease in autophagy levels at DEI 1 stage [31, 32]. From the second day of endoderm induction through the end of endoderm induction (DE), which coincided with the elimination of chir99021 in the media, a pronounced up-regulation in autophagy genes was observed. This was accompanied by conspicuous cell death as well as morphological changes which could be explained by the role of autophagy in tissue remodeling and structural changes [33]. High expression of *BECN1* in the MEI stage may signify its potential role in other autophagy-independent activities such as STAT3 phosphorylation [34, 35].

At DEI 1, DEI 2, and DE stages, by removal of chir99021 and addition of KSR and Activin A to the cell culture media, a gradual increase in *MAP1LC3B*, *SQSTM1/P62*, and *BECN1* expression was observed. This was accompanied by enhanced cell death and morphological changes which were in accordance with Vessoni et al.'s study[16].

In comparison with *MAP1LC3B*, *SQSTM1/P62*, and *BECN1*, the expression of *ATG5* was enhanced in EB and MEI and reduced significantly in the DE stage. This could be related to its complex interaction with other regulatory pathways, as such NF-κB and DNA repair pathways[36, 37].

The autophagy level was reduced and dropped to the lowest level during the rest of differentiation steps (PG, PF, and PE), compared to the iPSCs. The results indicated autophagy was activated at the definitive endoderm generation step and reached to a basic level during last steps of differentiation as it was also reported by Pantovic et al., [38].

Finally, β-like cells revealed a slight increase in autophagy level compared to human islet cells. This might be related to the presence of resveratrol (RSV) in culture media until the end of differentiation induction process. The role of RSV in differentiation of stem cells into different cell lineages has been reported in prior studies and is known to induce autophagy [39, 40].

The analysis of LC3b-II protein expression which is considered the most important indicator of autophagy showed a strong correlation with autophagy gene expression data.

Overall, our study presented a time-dependent investigation of autophagy specific genes expression patterns during the differentiation induction of iPSCs toward insulin-producing β-like cells. We demonstrated that the expression of autophagy genes progressed to the highest levels during the most critical stage of differentiation i.e., definitive endoderm induction. Illumination of such expression patterns may be utilized in modifying autophagy processes in establishing more efficient differentiation induction strategies. Moreover, the autophagy gene expression pattern could be implicated in therapeutic procedures, such as many human diseases including diabetes and pancreatic cancer [41-43]. For example, by

generating more efficient insulin-producing β cells for transplantation, regulating β cell function in diabetic models by autophagy inducers, or suppressing pancreatic cancer stem cells using autophagy inhibitors [44, 45].

Our results revealed a multistep pattern of hiPSCs differentiation as demonstrated by the decreased mRNA and protein expression of autophagy genes in the early stages of differentiation (EB and MEI) and then increased at the definitive endoderm induction stages followed by a dynamic pattern toward the end of differentiation. These results demonstrated the involvement of autophagy during the differentiation of hiPSCs toward islet-like cells, especially during the early stages of differentiation rather than the later stages. This is the first report of its kind pertaining to the effect of autophagy in the differentiation of β-like cells. Further functional studies are needed to further define the precise role of autophagy and associated regulatory molecules in the differentiation of hiPSCs toward islet-like cells.

ACKNOWLEDGEMENTS

The authors are grateful to the Organ Transplant Research Centre, Shiraz University of medical sciences and Islamic Azad University of Marvdasht for their executive support of this project.

CONFLICTS OF INTEREST: None declared.

FINANCIAL SUPPORT: None.

REFERENCES

1. Glick D, Barth S, Macleod KF. Autophagy: cellular and molecular mechanisms. *J Pathol* 2010;**221**:3-12.
2. Dikic I, Elazar Z. Mechanism and medical implications of mammalian autophagy. *Nat Rev Mol Cell Biol* 2018;**19**:349-64.
3. Mizushima N, Komatsu M. Autophagy: renovation of cells and tissues. *Cell* 2011;**147**:728-41.
4. Wen X, Klionsky DJ. Autophagy is a key factor in maintaining the regenerative capacity of muscle stem cells by promoting quiescence and preventing senescence. *Autophagy* 2016;**12**:617-8.
5. Marino G, Niso-Santano M, Baehrecke EH, Kroemer G. Self-consumption: the interplay of autophagy and apoptosis. *Nat Rev Mol Cell Biol* 2014;**15**:81.
6. Harati-Sadegh M, Kohan L, Teimoori B, *et al*. The effects of placental long noncoding RNA H19 polymorphisms and promoter methylation on H19 expression in association with preeclampsia susceptibility. *IUBMB life* 2020;**72**:413-25.
7. Galluzzi L, Green DR. Autophagy-independent functions of the autophagy machinery. *Cell* 2019;**177**:1682-99.
8. Walker SA, Ktistakis NT. Autophagosome biogenesis machinery. *J Mol Biol* 2020;**432**:2449-61.
9. Al-Bari MAA. A current view of molecular dissection in autophagy machinery. *J Physiol Biochem* 2020;76:357-72.
10. Levine B, Kroemer G. Biological functions of autophagy genes: a disease perspective. *Cell* 2019;**176**:11-42.
11. Yamada K, Pomposelli T, Schuetz C, Wang P. A strategy to simultaneously cure type 1 diabetes and diabetic nephropathy by transplant of composite islet-kidney grafts. *Front Endocrinol* 2021;**12**:632605.
12. Wisel S, Gardner J, Roll G, *et al*. Pancreas-after-islet transplantation in nonuremic type 1 diabetes: a strategy for restoring durable insulin independence. *Am J Transplant* 2017;**17**:2444-50.
13. Liu G, David BT, Trawczynski M, Fessler RG. Advances in pluripotent stem cells: history, mechanisms, technologies, and applications. Stem Cell Rev Rep 2020;**16**:3-32.
14. Ghorbani-Dalini S, Azarpira N, Sangtarash MH, *et al*. Optimization of activin-A: a breakthrough in differentiation of human induced pluripotent stem cell into definitive endoderm. *3 Biotech* 2020;10:215.
15. Pezzolla D, López-Beas J, Lachaud CC, et al. Resveratrol ameliorates the maturation process of β-cell-like cells obtained from an optimized differentiation protocol of human embryonic stem cells. *PLoS One* 2015;**10**:e0119904.
16. Vessoni AT, Muotri AR, Okamoto OK. Autophagy in stem cell maintenance and differentiation. *Stem Cells Dev* 2011;**21**:513-20.
17. Sheng Q, Xiao X, Prasadan K, *et al*. Autophagy protects pancreatic beta cell mass and function in the setting of a high-fat and high-glucose diet. *Sci Rep* 2017;**7**:16348.
18. Kong F-J, Wu J-H, Sun S-Y, Zhou J-Q. The endoplasmic reticulum stress/autophagy pathway is involved in cholesterol-induced pancreatic β-cell injury. *Sci Rep* 2017;**7**:44746.
19. Riahi Y, Wikstrom JD, Bachar-Wikstrom E, *et al*. Autophagy is a major regulator of beta cell insulin homeostasis. *Diabetologia* 2016;**59**:1480-91.

20. Quan W, Hur K, Lim Y, *et al*. Autophagy deficiency in beta cells leads to compromised unfolded protein response and progression from obesity to diabetes in mice. *Diabetologia* 2012;**55**:392-403.

21. Tanemura M, Ohmura Y, Deguchi T, *et al*. Rapamycin causes upregulation of autophagy and impairs islets function both in vitro and in vivo. *Am J Transplant* 2012;**12**:102-14.

22. Ren L, Yang H, Cui Y, *et al*. Autophagy is essential for the differentiation of porcine PSCs into insulin-producing cells. *Biochem Biophys Res Commun* 2017;**488**:471-6.

23. Pokrywczynska M, Krzyzanowska S, Jundzill A, *et al*. Differentiation of stem cells into insulin-producing cells: current status and challenges. *Arch Immunol Ther Exp (Warsz)* 2013;**61**:149-58.

24. Segev H, Fishman B, Ziskind A, et al. Differentiation of human embryonic stem cells into insulin-producing clusters. *Stem Cells* 2004;**22**:265-74.

25. Jiménez-Moreno N, Stathakos P, Caldwell M, Lane J. Induced pluripotent stem cell neuronal models for the study of autophagy pathways in human neurodegenerative disease. *Cells* 2017;**6**:24.

26. Menendez JA, Vellon L, Oliveras-Ferraros C, *et al*. mTOR-regulated senescence and autophagy during reprogramming of somatic cells to pluripotency: a roadmap from energy metabolism to stem cell renewal and aging. *Cell Cycle* 2011;**10**:3658-77.

27. Yin Z, Pascual C, Klionsky DJ. Autophagy: machinery and regulation. *Microbial Cell* 2016;**3**:588.

28. Pérez-Plasencia C, López-Urrutia E, García-Castillo V, *et al*. Interplay between Autophagy and Wnt/β-catenin signaling in cancer: Therapeutic potential through drug repositioning. *Front Oncol* 2020;**10**:1037.

29. Lorzadeh S, Kohan L, Ghavami S, Azarpira N. Autophagy and the Wnt Signaling Pathway: A Focus on Wnt/β-catenin signaling. *Biochim Biophys Acta Mol Cell Res* 2020;**1868**:118926.

30. Yoshida Y, Soma T, Matsuzaki T, Kishimoto J. Wnt activator CHIR99021-stimulated human dermal papilla spheroids contribute to hair follicle formation and production of reconstituted follicle-enriched human skin. *Biochem Biophys Res Commun* 2019;**516**:599-605.

31. Evangelisti C, Chiarini F, Paganelli F, *et al*. Crosstalks of GSK3 signaling with the mTOR network and effects on targeted therapy of cancer. *Biochim Biophys Acta Mol Cell Res* 2020;**1867**:118635.

32. Chen L, Yang Y, Bao J, *et al*. Autophagy negative-regulating Wnt signaling enhanced inflammatory osteoclastogenesis from Pre-OCs in vitro. *Biomed Pharmacother* 2020;**126**:110093.

33. Vessoni AT, Muotri AR, Okamoto OK. Autophagy in stem cell maintenance and differentiation. *Stem Cells Dev* 2012;**21**:513-20.

34. Hu F, Li G, Huang C, *et al*. The autophagy-independent role of BECN1 in colorectal cancer metastasis through regulating STAT3 signaling pathway activation. *Cell Death Dis* 2020;**11**:1-13.

35. Tang F, Christofori G. The cross-talk between the Hippo signaling pathway and autophagy: implications on physiology and cancer. *Cell Cycle* 2020:**19**:2563-72.

36. Peng X, Wang Y, Li H, *et al*. ATG5-mediated autophagy suppresses NF-κB signaling to limit epithelial inflammatory response to kidney injury. *Cell Death Dis* 2019;**10**:1-16.

37. Maskey D, Yousefi S, Schmid I, *et al*. ATG5 is induced by DNA-damaging agents and promotes mitotic catastrophe independent of autophagy. *Nat Commun* 2013;**4**:1-14.

38. Pantovic A, Krstic A, Janjetovic K, *et al*. Coordinated time-dependent modulation of AMPK/Akt/mTOR signaling and autophagy controls osteogenic differentiation of human mesenchymal stem cells. *Bone* 2013;**52**:524-31.

39. Wang W, Zhang L-M, Guo C, Han J-F. Resveratrol promotes osteoblastic differentiation in a rat model of postmenopausal osteoporosis by regulating autophagy. *Nutr Metab (Lond)* 2020;**17**:1-10.

40. Marycz K, Houston J, Weiss C, *et al*. 5-azacytidine and resveratrol enhance chondrogenic differentiation of metabolic syndrome-derived mesenchymal stem cells by modulating autophagy. *Oxid Med Cell Longev* 2019;**2019**: 1523140.

41. Yao D, GangYi Y, QiNan W. Autophagic dysfunction of β cell dysfunction in type 2 diabetes, A Double-edged Sword Autophagic Dysfunction in Type 2 Diabetes. *Genes Dis* 2020;8:438-47.

42. Mollinedo F, Gajate C. Novel therapeutic approaches for pancreatic cancer by combined targeting of RAF→ MEK→ ERK signaling and autophagy survival response. Ann Transl Med 2019;**7**:S153

43. Bryant KL, Der CJ. Blocking autophagy to starve pancreatic cancer. Nat Rev Mol Cell Biol 2019;**20**:265.

44. Barnhart BC, Simon MC. Metastasis and stem cell pathways. *Cancer Metastasis Rev* 2007;**26**:261-71.

45. Salimi S, Harati-Sadegh M, Eskandari M, Heidari Z. The effects of the genetic polymorphisms of antioxidant enzymes on susceptibility to papillary thyroid carcinoma. *IUBMB life* 2020;**72**:1045-53.